

# Object Selectivity of Local Field Potentials and Spikes in the Macaque Inferior Temporal Cortex

Gabriel Kreiman,<sup>1,2,3,4,7,\*</sup> Chou P. Hung,<sup>1,2,4,7</sup>  
Alexander Kraskov,<sup>5</sup> Rodrigo Quian Quiroga,<sup>6</sup>  
Tomaso Poggio,<sup>1,2,3,4</sup> and James J. DiCarlo<sup>1,2,4</sup>

<sup>1</sup>McGovern Institute for Brain Research

<sup>2</sup>Center for Biological and Computational Learning

<sup>3</sup>Computation and Systems Biology Initiative

<sup>4</sup>Department of Brain and Cognitive Sciences

Massachusetts Institute of Technology

Cambridge, Massachusetts 02139

<sup>5</sup>Division of Biology

California Institute of Technology

Pasadena, California 91125

<sup>6</sup>Department of Engineering

University of Leicester

Leicester, LE1 7RH

United Kingdom

## Summary

Local field potentials (LFPs) arise largely from dendritic activity over large brain regions and thus provide a measure of the input to and local processing within an area. We characterized LFPs and their relationship to spikes (multi and single unit) in monkey inferior temporal cortex (IT). LFP responses in IT to complex objects showed strong selectivity at 44% of the sites and tolerance to retinal position and size. The LFP preferences were poorly predicted by the spike preferences at the same site but were better explained by averaging spikes within  $\sim 3$  mm. A comparison of separate sites suggests that selectivity is similar on a scale of  $\sim 800$   $\mu\text{m}$  for spikes and  $\sim 5$  mm for LFPs. These observations imply that inputs to IT neurons convey selectivity for complex shapes and that such input may have an underlying organization spanning several millimeters.

## Introduction

Although spiking activity has been extensively studied throughout the different subdivisions of the primate visual cortex, spikes only provide information about the outputs of neurons in an area. In this study, we focus on another measure of neuronal activity, the local field potential (LFP), which is thought to arise largely from dendritic activity and therefore reflects the inputs to and local processing within a brain area (Logothetis, 2003; Mitzdorf, 1985). We characterized LFP responses and their relationship to spiking activity in monkey inferior temporal cortex (IT). IT is critical for visual object recognition (for reviews, see Logothetis and Sheinberg, 1996; Tanaka, 1996). IT neurons respond to complex objects (Gross et al., 1972), and nearby neurons show similar stimulus preferences (Fujita et al., 1992; Tanaka, 2003; Wang et al., 1996). It is thought that the selectivity of IT

neurons arises from nonlinear transformations iterated along the cortical ventral visual hierarchy (Felleman and Van Essen, 1991; Fukushima, 1980; Gross, 1994; Riesenhuber and Poggio, 1999). The transformation of visual representations from one cortical stage to the next constitutes one of the crucial computations performed in cortex and requires understanding how the dendritic input (presumably related to the LFPs) is transformed into the spiking output (Kreiman, 2004). A simultaneous examination of both spiking activity and LFPs could provide a better understanding of the organization of the inputs to IT neurons in particular and of the relationship between spikes and LFPs in cortex in general.

Cortical evoked potentials from electroencephalograms were obtained as early as the 1930s, and intracortical recordings of LFPs date back to the 1950s (Haberly and Shepherd, 1973; Mitzdorf, 1985). Nevertheless, while the biophysical origin of spiking activity is well understood (Hodgkin and Huxley, 1952; Koch, 1999), less is known about the origin of LFPs. Spiking activity is obtained by high-pass filtering the extracellular voltage (typically above  $\sim 300$  Hz) and isolating spike waveforms from the ensuing signal. In contrast, the LFP is the signal obtained by low-pass filtering the extracellular voltage (here, below 300 Hz and excluding DC). Simultaneous studies of spiking activity and LFPs, combined with current source-density analysis, suggest that the LFPs arise from the combined activity of large numbers of neurons distributed over a large region of cortex (Mitzdorf, 1985). The primary component measured by the LFP in cortex is thought to be the excitatory postsynaptic potentials of dendrites plus afterhyperpolarizing potential and afterdepolarizing potential (Logothetis, 2003; Mitzdorf, 1985). The synaptic input to IT cells is largely composed of (1) feedforward signals from earlier areas, such as V4, (2) feedback signals from areas such as prefrontal cortex and the medial temporal lobe, and (3) local connectivity. Throughout the text, we refer to these three sources as “synaptic input” to IT cells.

The LFP constitutes a collective property of a neuronal ensemble and not a property of individual neurons. Studies of the spiking responses from individual neurons show that nearby IT neurons within 200 to 500  $\mu\text{m}$  show a preference for similar objects (Fujita et al., 1992; Gochin et al., 1991; Wang et al., 1996). It is tempting to assume that spatial patterns of object selectivity revealed by spatially coarse measures such as LFPs, evoked response potentials in the occipito-temporal lobe of human patients (Allison et al., 1994), optical imaging (Wang et al., 1996), and fMRI BOLD (Grill-Spector and Malach, 2004; Haxby et al., 2001; Kanwisher et al., 1997; Logothetis, 2003) are somehow related to the proposed topographical organization of spiking activity in cortex. However, the relationship among such signals is poorly understood, particularly in IT cortex.

Here we studied the relationship of the ensemble synaptic input to IT and the spiking output. We observed that almost half of the sites showed LFP object-selective responses and that selectivity was tolerant of changes in the scale and position of the stimuli as shown previously

\*Correspondence: kreiman@mit.edu

<sup>7</sup>These authors contributed equally to this work.

for spiking activity (Ito et al., 1995; Logothetis and Sheinberg, 1996; Sato et al., 1980; Schwartz et al., 1983; Tanaka, 1996; Wallis and Rolls, 1997). Although both LFPs and spikes showed robust selectivity, the LFP-determined object preferences at each IT site were poorly predicted by the spiking activity at the same site. The LFP could be better explained by averaging spiking activity within  $\sim 3$  mm around the LFP. Consistent with this, we found that LFP object preferences at pairs of recording sites remained similar until the sites were several millimeters apart. To the extent that LFPs reflect synaptic input activity, these observations provide evidence that synaptic inputs to IT convey position- and size-tolerant selectivity for complex shapes and that such synaptic inputs may have an underlying spatial organization on a spatial scale spanning several millimeters.

## Results

We recorded multi-unit activity (MUA) and local field potentials (LFPs) from the same electrode, and only recordings that passed stability requirements were accepted for further analysis (Experimental Procedures). We performed spike sorting on the MUA to obtain single-unit activity (SUA) (Quiari Quiroga et al., 2004). We recorded reliable extracellular MUA from 364 sites in 122 penetrations and LFPs (1–300 Hz frequency band) from 315 sites in 93 penetrations made across the IT cortex in three hemispheres of two macaque monkeys by the use of single electrodes (Experimental Procedures) while the animals passively viewed 77 complex objects (see Figure S1 in the Supplemental Data available online). Images included human and monkey faces, toys, foodstuffs, vehicles, cats, and shape contours and were presented one at a time at the center of gaze while the animal passively fixated. Images were presented at a rate of five per second (100 ms presentation duration, 100 ms interval between presentations). Spike counts from MUA or SUA showed stimulus selectivity beginning  $\sim 100$  ms after stimulus onset, as reported previously (DiCarlo and Maunsell, 2000; Gross et al., 1972; Logothetis and Sheinberg, 1996; Perrett et al., 1982; Schwartz et al., 1983; Tanaka, 1996).

### Local Field Potentials in IT Are Stimulus Selective

We asked whether LFPs in IT show selectivity for visually presented stimuli. A representative example of the LFP responses from a single site is shown in Figure 1. The gray traces next to each stimulus show the time-locked LFP waveforms produced by that stimulus (ten repetitions for each image), and the thick red line shows the average of those traces. The LFP signal showed a strong modulation for some of the stimuli. The responses shown in Figures 1, 2, and 4 are typical of the LFP signals we examined in this study: the first two principal components of the LFP signals accounted for more than 80% of the variance and consisted of biphasic or triphasic potential changes beginning  $\sim 100$  ms after stimulus onset. The LFP signal was dominated by low-frequency power; the 1–40 Hz band contained  $82\% \pm 22\%$  (mean  $\pm$  SD) of the total signal power (Figure S2A).

To quantify the stimulus selectivity in the LFPs, we first examined the signal power for each individual LFP

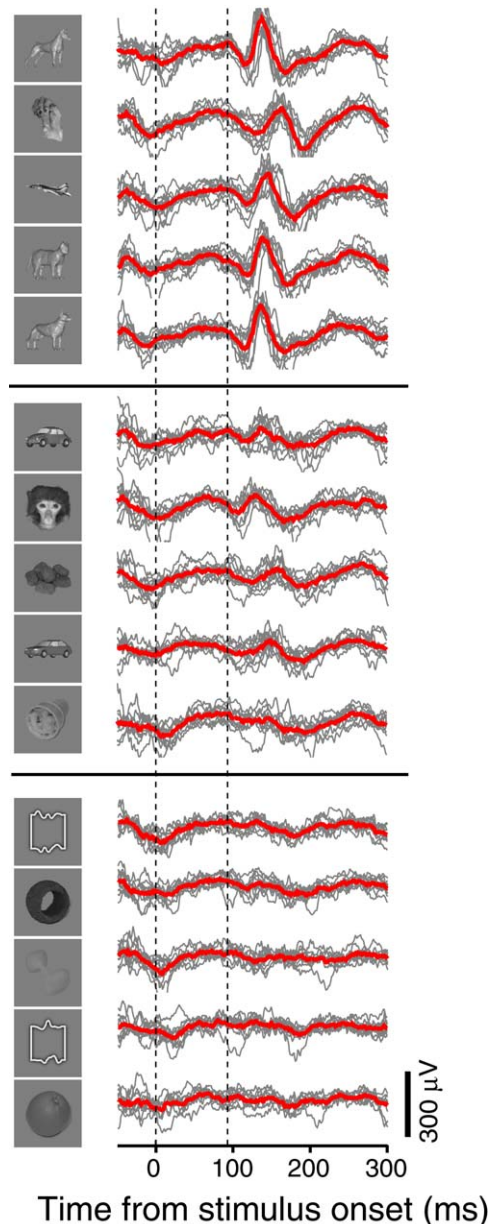


Figure 1. Example of Selectivity in LFPs

Example of the LFP responses at one IT recording site to 15 different images (the responses to all 77 images for this site are shown in Figure S1). The gray lines show the LFP response to each of the ten repetitions of each stimulus aligned at the time of stimulus onset (the raw signal is low-pass filtered at 300 Hz, and the DC component is removed). The thick red line shows the average LFP waveform. The vertical dashed lines denote stimulus onset and offset. The images are sorted here in decreasing order of the LFP response magnitude showing the top five images (top), the worst five images (bottom), and five intermediate images (middle).

trace (each gray line in Figure 1) in each of several frequency bands in the time window from 100 to 200 ms after stimulus onset (Experimental Procedures). This analysis window was chosen so as to maximize the proportion of selective sites for MUA and LFPs (Figure S3). Unless stated otherwise, we here define the “LFP response” to each image as the total power over the entire 1–300 Hz range. To assess the stimulus selectivity in

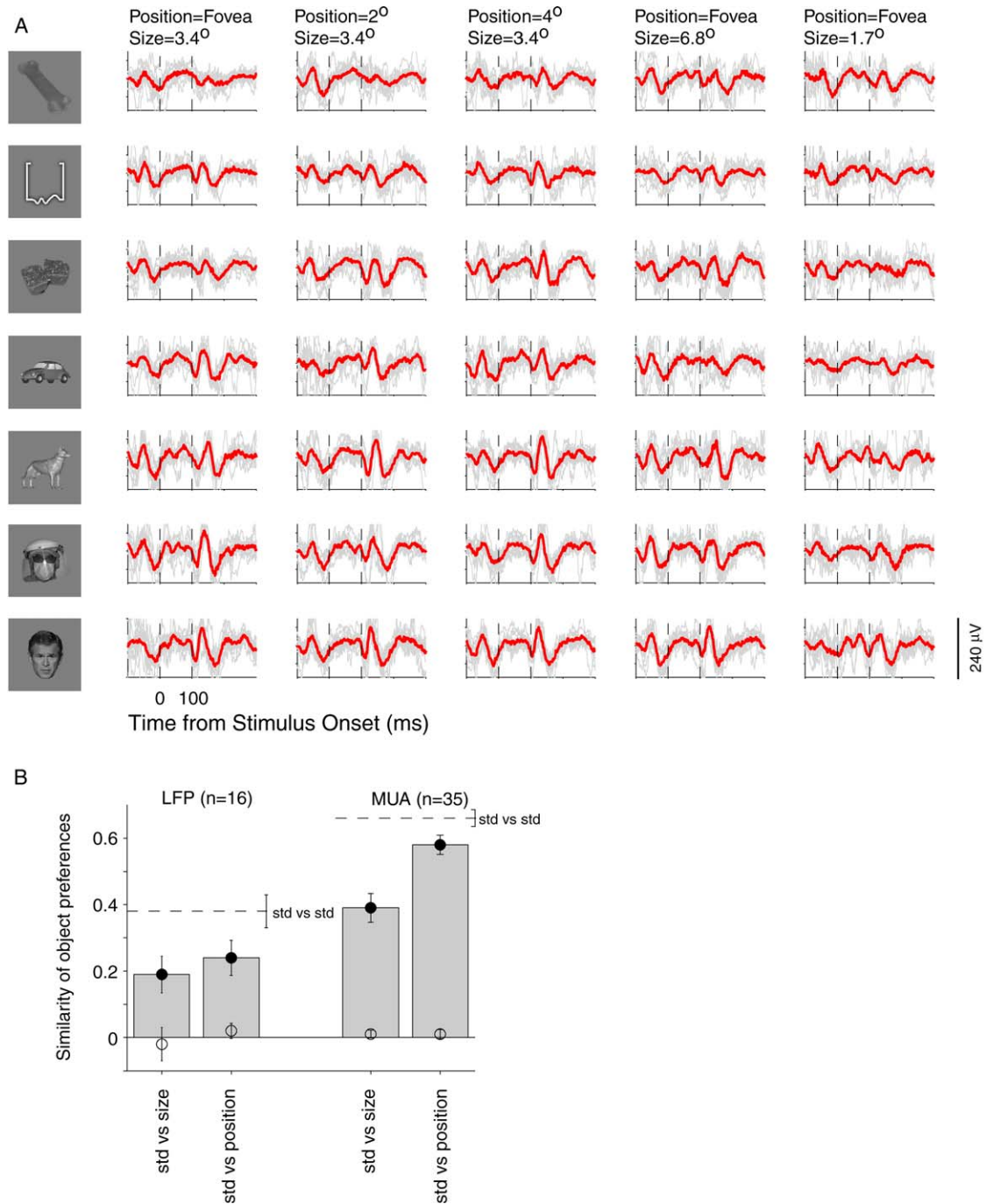


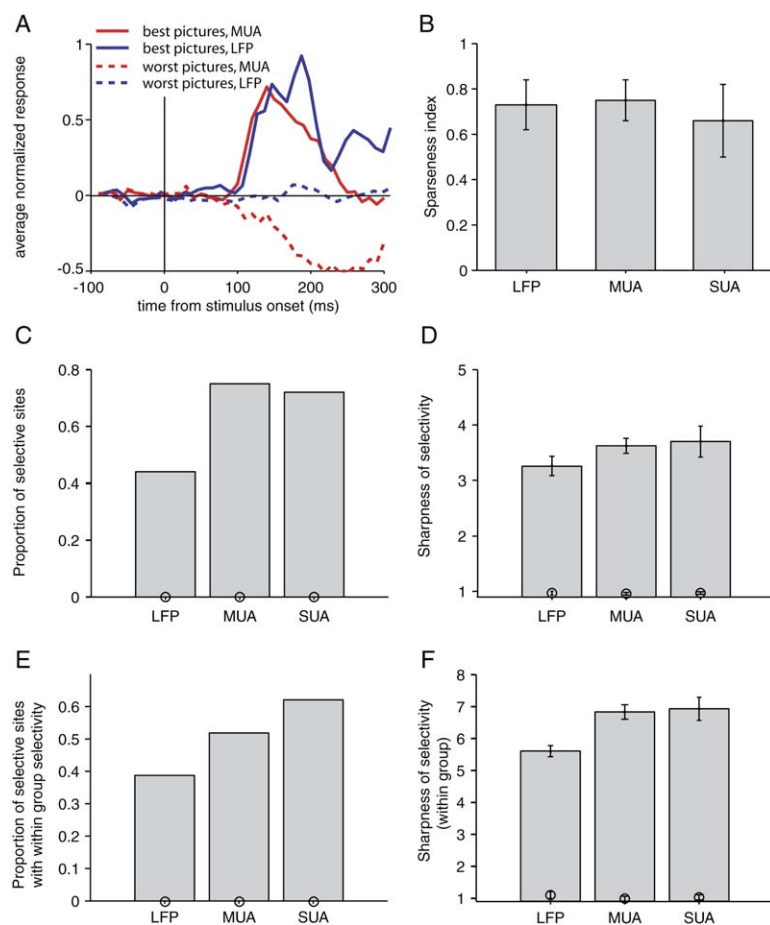
Figure 2. Invariance of LFP Responses

(A) Example showing the LFP responses at one site to seven stimuli at the standard position and size (center of gaze, 3.4°), shifted positions at the standard size (shift of 2° and 4° along contralateral horizontal meridian), and scaled versions at the center of gaze (6.8° and 1.7°). The format follows the conventions in Figure 1.

(B) Similarity of object preferences for selective sites across sizes and positions for LFP (n = 16) and MUA (n = 35). We computed the Pearson correlation coefficient between the responses to the 77 images at the standard position and size (see above) versus the 77 images at the shifted position (“std vs. position,” average over the two different positions) or scaled version (“std vs. size,” average over the two sizes). The empty circles show the correlation coefficients during the 100 ms before stimulus onset, and the filled circles correspond to the correlation coefficients during the 100–200 ms interval after stimulus onset. For comparison, we also computed the correlation coefficient between odd and even trials for the standard size and position (“std vs. std”). If the responses showed complete invariance, the filled circles would fall on the dashed line; if they showed no invariance, they would fall along the zero line. Error bars show SEM.

the LFPs, we performed a one-way ANOVA on the LFP responses from each site, with stimulus identity as the main factor. Instead of comparing against a baseline,

the ANOVA compared the responses across different stimuli in the same presentation window (Keyesers et al., 2001). The site shown in Figure 1 yielded  $p < 0.001$ ,



(F) Sharpness of selectivity (mean ± SD) for those sites that showed *within*-group selectivity (E) for LFP (n = 77), MUA (n = 213), and SUA (n = 75). The selectivity sharpness (y axis) was restricted to each of the eight possible groups and was defined as the ratio of the variance across pictures to the variance within pictures.

showing a statistically significant differential response to distinct stimuli. A post hoc t test comparison against the baseline, defined as the 100 ms before stimulus onset, further showed selectivity for several images ( $p < 0.001$ , marked by \* in Figure S1). We found that 139 of the 315 sites (44%) produced LFP responses with significant stimulus selectivity (one-way ANOVA,  $p < 0.001$ ,  $df = 76$ ). This is remarkable because it suggests that a spatially coarse electrophysiological measure that likely spans large numbers of neurons shows stronger responses for some stimuli than others. Examples of LFP data from such selective sites are shown in Figures 1, 2, and 4. Selectivity was also observed for other definitions of LFP response, including the range of the LFP signal (max-min) (Mehring et al., 2003), the power in different frequency bands (Figure S2B), and different analysis time windows (Figure S3).

We briefly describe here several additional controls to verify the LFP stimulus selectivity (see Experimental Procedures for further details). Briefly, the LFP signal showed a latency of ~100 ms (Figure 3A), which is similar to that of spiking activity (DiCarlo and Maunsell, 2000; Richmond et al., 1983). None of the sites showed selectivity with the same analysis applied to the LFP data in the control interval before stimulus onset (-100

Figure 3. Overall Comparison of Spiking and LFP Responses

(A) Average time course of the MUA responses (red, n = 279 MUA-selective sites) and LFP responses (blue, n = 139 LFP-selective sites). For each site, we took the activity for the best five stimuli (solid trace) and the worst five stimuli (dashed trace). The activity was binned (bin size = 10 ms, spike count for MUA and signal power for LFP), the response to the “blank” image was subtracted, and the resulting signal was normalized by the 95th response percentile (similar to normalizing by the maximum, but more robust). The resulting response waveform was then averaged over all the included sites.

(B) Sparseness index (mean ± SD) for LFP, MUA, and SUA (Experimental Procedures). This index has a maximum value of 1.

(C) Overall proportion of selective sites for LFP, MUA, and SUA. Selectivity here was defined by a one-way ANOVA for the 77 images, with picture identity as the main factor,  $p < 0.001$ . In this and subsequent subplots, the empty circles show the same analysis using the 100 ms before stimulus presentation.

(D) Sharpness of selectivity (mean ± SD) for selective sites for LFP (n = 139), MUA (n = 279), and SUA (n = 138). The selectivity sharpness (y axis) was defined as the ratio of the variance across pictures to the variance within pictures (as used in the ANOVA analysis).

(E) Proportion of the selective sites that showed selectivity *within* at least one of the eight groups of stimuli (Experimental Procedures). Selectivity here was defined by a one-way ANOVA for all the images *within* a group, with picture identity as the main factor,  $p < 0.001$ .

to 0 ms). We also recorded spiking and LFP “activity” at 18 additional sites outside IT cortex (in the white matter just above IT cortex or in the striatum) while presenting the same stimuli. None of these sites showed selective responses, distinguishing our observations from scalp recordings. To examine whether the LFP selectivity was due to low-level image properties (e.g., total luminance, etc.), we first repeated the selectivity analysis after excluding images with low contrast at the center of gaze, including the objects consisting of white contours (12% of the images). The proportion of selective sites was only slightly lower (38%; cf. 44% for the full stimulus set). We also quantified how much of the LFP selectivity could be explained by each of 16 low-level image properties (Experimental Procedures). The image property that accounted for the largest amount of the variance was the standard deviation of the pixel intensities, which explained, on average, only 7% of the LFP response variance. Thus, LFP responses showed robust stimulus selectivity that could not be simply explained by low-level image properties.

Both the MUA and LFP responses extended well beyond stimulus offset (Figure 1 and Figure S3). Due to the short presentation times, the responses continued up to and overlapped the presentation of the following

stimulus. To better measure the duration of the responses, we also recorded from 24 additional sites where the stimuli were presented for 200 ms, and there was a 300 ms blank interval between stimuli. For the LFPs, five sites (21%) showed a selective response 400 ms after stimulus onset, suggesting that the duration of the LFP response can last several hundred milliseconds.

To assess whether the LFP was only coarsely selective to very distinct sets of stimuli (such as faces versus cars) or was also selective to finer differences among the stimuli, we performed a one-way ANOVA *within* each one of eight groups of stimuli: toys, foodstuffs, human faces, monkey faces, body parts, vehicles, white boxes, and cats/dogs (Figure S1). Out of the 315 sites, 77 (24%) showed selectivity ( $p < 0.001$ ) within at least one of these groups (only 1/315 sites showed such within-group selectivity during the control time interval before stimulus onset). Selective responses were nonuniformly distributed across our set of stimuli. The strongest effect (both for MUA and LFPs) was that none of the sites showed selectivity within the set of white contours. However, our conclusions remain unaltered upon removal of these object images (see above, Figure 5B, and the Supplemental Data). To consider the selectivity of the MUA and LFP signals beyond the common preferences across multiple sites, we subtracted the average signal across all sites from the responses and repeated the selectivity analysis. This reduced the proportion of selective sites to 73% for MUA and 31% for LFPs (cf. 77% and 44%, respectively, for the raw signals).

A hallmark of spiking activity in IT is the robustness to large changes in the visual input (Ito et al., 1995; Logothetis and Sheinberg, 1996; Sato et al., 1980; Schwartz et al., 1983; Tanaka, 1996; Wallis and Rolls, 1997). To examine whether LFP responses also showed such tolerance, we recorded from 45 additional sites to examine the effect of changes in object position and size. In addition to the standard object position (center of gaze) and size ( $3.4^\circ$ ), the same 77 objects were also presented at two new positions at the same size ( $2^\circ$  and  $4^\circ$  from the center of gaze along the contralateral horizontal meridian) and two new sizes at the center of gaze (half the size and twice the original size). Object-selective LFP sites often showed tolerance to these changes in object position and scale (Figure 2A shows an example recording site). To quantify the degree of tolerance, we computed the Pearson correlation coefficient between the 77 responses at the standard position and size and the 77 responses at the other positions or sizes. Figure 2B shows the average degree of tolerance to scale and position changes. Although both the spike and LFP signals showed trial-to-trial variability, a statistical comparison against chance levels (Figure 2B, filled versus empty circles) shows that the results are highly significant (t test,  $p < 10^{-4}$ ).

### Comparison of Spiking and LFP Selectivity

How does the stimulus selectivity of spiking activity compare to that of LFP responses? We directly compared the selectivity of spikes and LFPs at each site. To the extent that we could measure, the latency of selective spiking responses was approximately similar to the latency of selective LFP responses (Figure 3A). The fraction of stimuli that drove responses, as measured

by the sparseness index (Experimental Procedures), was also similar for MUA and LFP responses and slightly lower for SUA (Figure 3B). However, across all sites, there was no correlation between the sparseness index for MUA and LFP ( $\rho = -0.11$ ). The overall proportion of sites that showed selectivity was higher for MUA or SUA than for LFPs (Figure 3C). The proportion of sites that showed selectivity *within* groups of stimuli and the fraction of the selective sites that showed within-group selectivity were also higher for spikes (Figure 3E). Of the 364 sites with MUA, 279 (77%) showed significant selectivity (ANOVA of the spike counts from 100 to 200 ms after stimulus onset,  $p < 0.001$ ) compared to 44% for LFPs as reported above. Of 249 IT sites where both stable MUA and LFP data were obtained, 90 sites showed MUA-determined selectivity without LFP-determined selectivity ( $p < 0.001$ ), only 14 sites showed LFP selectivity without MUA selectivity, and 87 sites (35%) showed both MUA and LFP selectivity.

We also looked at an index of the sharpness of stimulus selectivity: the ratio of the variance of the response across images to the variance of the response within images ( $r_v$ , as used in the ANOVA analysis). The value of  $r_v$  was higher for MUA ( $3.6 \pm 2.1$ , mean  $\pm$  SD) than for LFPs ( $3.1 \pm 1.5$ ), indicating that IT sites show sharper MUA-determined stimulus selectivity than LFP-determined selectivity (Figure 3D, t test,  $p < 0.01$ ). We found only a weak correlation ( $\rho = 0.11$ ) between the sharpness of MUA-determined and LFP-determined selectivity, indicating that the presence of MUA selectivity at a site is only a weak predictor of LFP selectivity at the same site (Figure S4). Within-group selectivity was also significantly sharper for spikes than for LFPs (Figure 3F, t test,  $p < 0.01$ ).

How do the MUA-determined stimulus preferences at each selective site compare to the LFP-determined stimulus preferences? Figure 4 shows recordings from four example sites that illustrate the range of relationships seen across the population of sites. In some cases, the same stimuli produced an enhancement in both the MUA and the LFP signals. For example, Figure 4A shows responses from a site that displayed a strong enhancement in both the LFP and MUA responses for images of cats and dogs. Figure 4E compares, for this site, the average spike count to the average LFP response for all 77 stimuli ( $\rho = 0.71$ ). More typically, however, as the example sites in Figures 4B–4D illustrate, we observed cases where some stimuli produced an enhancement in the MUA signal without concomitant changes in the LFP response and vice versa. For example, the site illustrated in Figure 4B showed an enhanced LFP response to the presentation of an image of food (peanuts) but little MUA response to the same image. In contrast, the same site showed no clear LFP response to the presentation of a human face but a robust spike response (Figure 4F,  $\rho = 0.06$ ). Similarly, Figure 4C shows a site with a strong spiking response to an image of an apple and no response to a masked face, while the LFP for this site showed a vigorous response to the masked face and no response to the apple. The site shown in Figure 4D also shows different spike and LFP stimulus preferences (Figure 4G,  $\rho = -0.50$ ).

To quantify the similarity of the stimulus preferences seen in the MUA and LFP, we examined all 87 sites

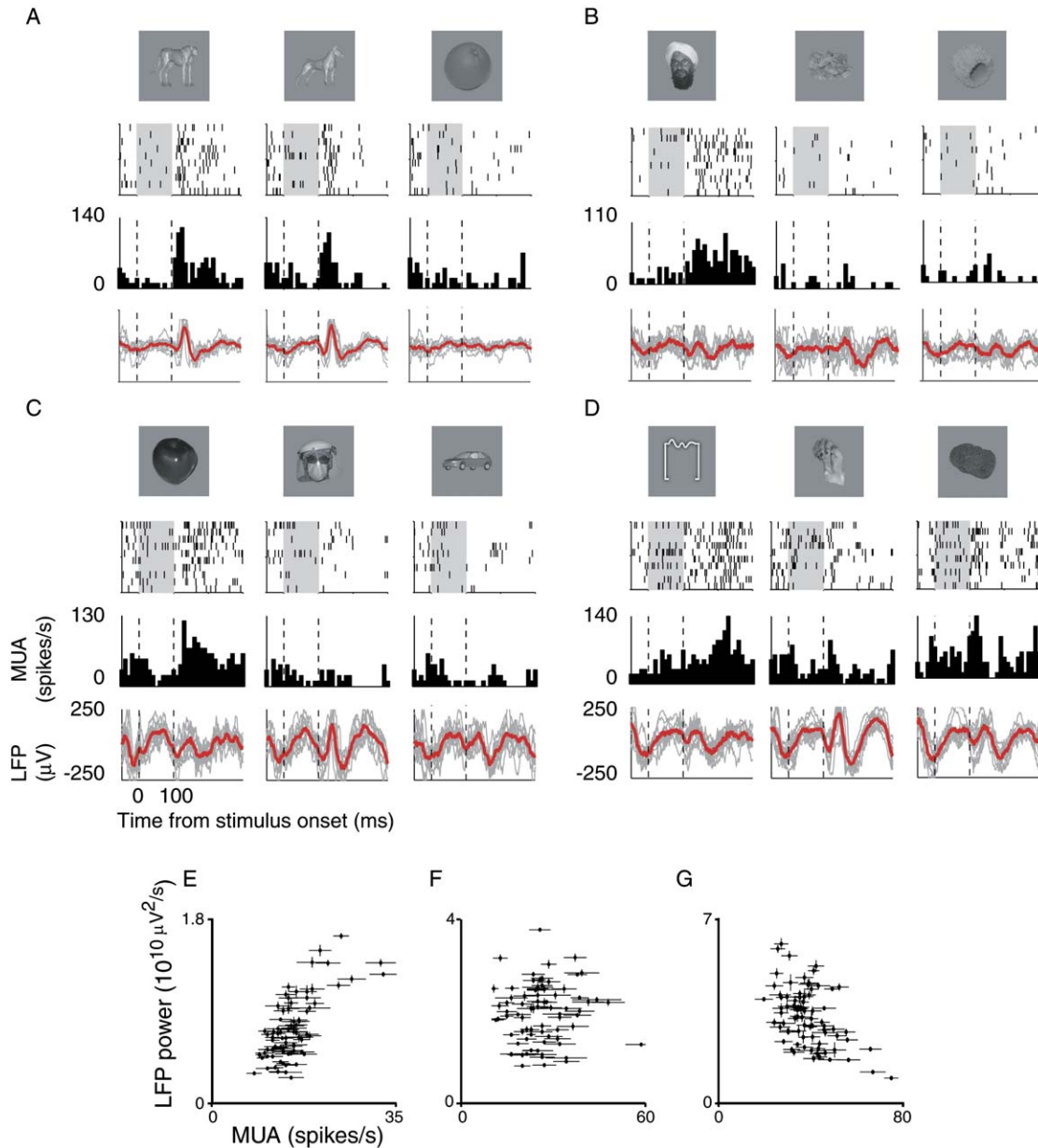


Figure 4. Four Examples of MUA and LFP Responses

(A–D) Examples of the MUA and LFP responses at four sites to three images. For each site, we show the image eliciting the largest MUA response (left, defined by the spike count in the 100–300 ms after stimulus onset), the image eliciting the largest LFP response (center, defined by the total power from 1–300 Hz in the same time interval), and a randomly chosen image (right). The MUA responses are shown as raster plots where each row shows a separate image repetition and each tick indicates a spike (aligned to stimulus onset). The gray box denotes the stimulus presentation period (93 ms). Below the raster plot we show the peristimulus time histogram (PSTH), bin size = 10 ms. The LFP responses are shown in the bottom part of each subplot, using the same format as in Figure 1. The dashed lines indicate the stimulus presentation time. The average MUA and LFP responses to each of the 77 images for sites (A), (B), and (D) are shown as scatter plots in (E)–(G). (E–G) Data from three example sites showing the relationship of LFP power (ordinate) and MUA spike count (abscissa) for each of the 77 images. The SEM error bars for the MUA and LFP responses are shown for each image. The data shown in panels (E)–(G) correspond to the sites shown in parts (A), (B), and (D), respectively. The correlation coefficients were 0.71 (A), 0.06 (B), and  $-0.50$  (D). These values are indicated by the arrows in the distribution shown in Figure 5A.

that showed both significant MUA and LFP selectivity. We first computed the degree of overlap between the ten most-preferred stimuli determined by either MUA or LFP. The number of stimuli in common for these was, on average,  $1.7 \pm 1.4$  (mean  $\pm$  SD), which was only slightly greater than the number expected by chance ( $1.3 \pm 1.0$ , t test,  $p < 0.01$ ). We next examined stimulus preference

similarity by computing the Pearson correlation between the MUA responses and the LFP responses across all 77 stimuli for each of the sites (e.g., Figures 4E–4G). Overall, we observed a wide, unimodal distribution of correlation values (Figure 5A). The distribution revealed a significant but small average correlation between the MUA and LFP stimulus preferences ( $\rho = 0.19 \pm 0.21$ ,

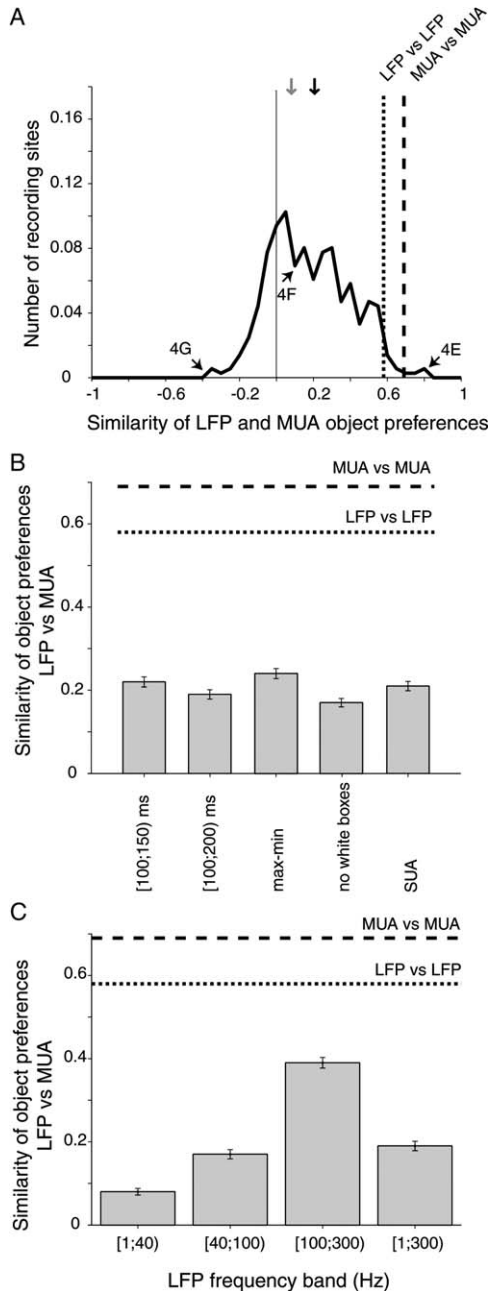


Figure 5. Similarity of MUA-Determined and LFP-Determined Stimulus Preferences

(A) Distributions of Pearson correlation coefficients between MUA and LFP responses in the stimulus interval (100–200 ms after stimulus onset) obtained from the 87 sites with significant MUA and LFP selectivity. The arrows denote the mean correlation coefficient for the stimulus interval (black,  $0.19 \pm 0.21$ ) and the interval before stimulus onset (gray,  $0.06 \pm 0.14$ ). For comparison, in this and subsequent subplots we show the mean correlations between responses determined from even-numbered stimulus repetitions and odd-numbered stimulus repetitions (dashed line is MUA versus MUA; dotted line is LFP versus LFP, both were corrected for number of trials, see Experimental Procedures). We also marked the three examples from Figure 4.

(B) Similarity of object preferences between spiking activity and LFP for different definitions of spike and LFP response. The first two bars show the correlation coefficients when the LFP response was defined as the power in the 100–150 and 100–200 ms window after stimulus onset. “max(LFP)–min(LFP)” denotes the amplitude of the

mean  $\pm$  SD for the stimulus interval; Spearman correlation coefficients yielded similar results:  $\rho = 0.20 \pm 0.21$ ). Although small, this correlation was dependent on the visual stimulus presentation, as evidenced by the even lower correlation during the 100 ms interval before stimulus onset ( $\rho = 0.06 \pm 0.14$ , mean  $\pm$  SD). This low level of similarity in the stimulus preferences cannot simply be explained by variability in the responses, because the similarities of stimulus preferences observed in the MUA or LFP determined from comparing two halves of the data (even and odd numbered presentations) were much larger (after correction for the number of trials,  $0.69 \pm 0.22$ , MUA versus MUA;  $0.58 \pm 0.25$ , LFP versus LFP; mean  $\pm$  SD, see Figure 5A and Experimental Procedures).

We also considered several other possible comparisons between the stimulus preferences of spiking activity and LFPs. Instead of considering the LFP power and spike counts in the 100–200 ms interval after stimulus onset, we also considered the response in other possible intervals. Figure 5B shows the corresponding correlation coefficients for the 100–150 ms interval. The 100–300 ms interval showed a significantly weaker correlation (t test,  $p < 0.01$ ), indicating that spiking responses and LFP responses were even more dissimilar 200 ms after stimulus onset. Given that the LFP and MUA activity have different timescales (Figure S3), we also compared their object preferences by using different response intervals for each signal; the highest correlation coefficient that we observed was 0.24, suggesting that the weak similarity of MUA and LFP preferences is not due to the different timescales. The strongest correlation coefficient for 24 additional sites where stimuli were presented for 200 ms was 0.25. We made similar observations when using the range (max–min) of the LFP signal instead of the power (Figure 5B). Some images had no contrast at the center (e.g., white box stimuli, Figure S1); removing these images from analysis did not increase the correlation between spiking activity and LFPs (Figure 5B). Finally, the correlation between SUA and LFP was similarly weak (Figure 5B). Thus, these observations show that at each site there was a statistically significant but weak relationship between the object preferences of spikes and LFPs.

To examine the relationship of spike and LFP stimulus preferences more closely, we computed the correlation coefficient between the power in different LFP frequency bands and the MUA spike counts (Figure 5C). The stimulus preferences of the LFP lower-frequencies bands (<40 Hz) showed only a weak correlation with the MUA stimulus preferences. This is consistent with our observations that most of the LFP power was <40 Hz and that the total LFP power stimulus preferences were only weakly correlated with the MUA preferences.

LFP signal in the 100–200 ms interval. “no white boxes” denotes the correlation coefficient after removing the white box stimuli (Figure S1 and Experimental Procedures). The last column shows the correlation coefficient between LFP and SUA. Error bars denote SEM.

(C) Mean correlation coefficient between the MUA and LFP responses for all 77 pictures for different frequency bands of the LFP response (Experimental Procedures). The value for the 1–300 Hz frequency band corresponds to the mean of the distribution in panel (A). Error bars denote SEM.

In contrast, the 100–300 Hz LFP frequency band yielded a significantly higher similarity with the MUA-determined stimulus preferences ( $\rho = 0.39 \pm 0.24$ , mean  $\pm$  SD). This higher similarity is not surprising, because this frequency band abuts the low end of the MUA band and is therefore the LFP band that is most likely to contain some components of the spike waveforms themselves. The results shown in Figure 5 were essentially unaffected by the choice of statistical threshold used to define selective sites; similarity measures based on the subsets of stimuli that were significantly responsive at each site produced similar results (data not shown).

In sum, all of our analyses revealed a significant but weak similarity in the stimulus preferences of the spiking response and the LFP response below 40 Hz at each site. This result is surprising given that both measures were recorded simultaneously from the same electrode, but it is consistent with the hypothesis that the MUA and the LFP are reporting different but related aspects of IT cortical function (Logothetis, 2003; Mitzdorf, 1985).

### Similarity of Stimulus Selectivity at Nearby Recording Sites

The LFP (particularly the lower frequencies) constitutes an ensemble measure that pools information over a large cortical region compared to spikes (Logothetis, 2003; Mitzdorf, 1985). Therefore, we asked whether the LFP signal could be related to the spikes over a larger, nearby cortical area. To evaluate this hypothesis, we built a simple model whereby we compared the LFP response at each recording site with a signal composed of the average of spiking activity over all recorded sites within a given distance of that LFP recording site. This average spiking signal was still stimulus selective. Furthermore, this average signal showed a stronger correlation to the LFP selectivity ( $0.35 \pm 0.25$ , mean  $\pm$  SD, Figure 6, filled squares) than that obtained from the spikes at the LFP recording site (Figure 5A and distance = 0 point in Figure 6). This does not imply that individual sites farther away from the electrode show a stronger correlation (individual sites farther away from the LFP recording site showed a weaker correlation); it is the average model signal that shows a stronger correlation with the LFP signal. The model also shows that the inclusion of spiking sites beyond  $\sim 3$  mm of the electrode does not further explain the selectivity of the LFP response. If this improvement in correlation were related to the spatial structure of cortical selectivity in IT, then one could expect that more remote sites would show a weaker correlation with the LFP. Thus, we repeated the analysis but averaging only those sites that were beyond a given distance from the LFP recording site. We found that the correlation with the LFP responses began to decrease when only spiking sites more than  $\sim 3$  mm away from the LFP recording site were included (Figure 6, empty squares). Similarly, when we averaged only sites within an annulus around the electrode, we found that the correlation decreased gradually as the radius of the annulus was made larger beyond 6 mm (data not shown). Taken together, these analyses indicate that the LFP stimulus selectivity in IT is best explained (but not fully explained) by averaging spiking activity within  $\sim 3$  mm of the electrode.

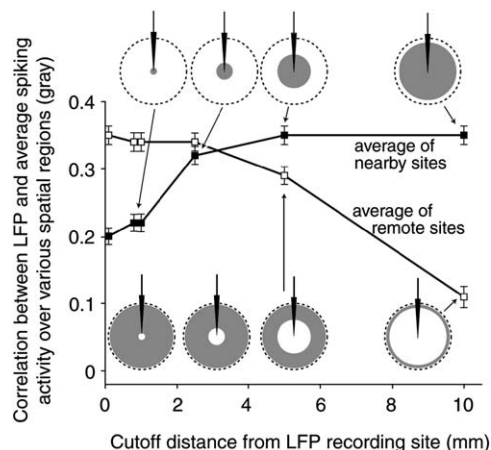


Figure 6. Comparison of LFP Response against Simple Model  
For each LFP recording site, we built a simple model whereby we averaged the MUA activity of multiple sites surrounding (filled squares) or remote (open squares) to each LFP recording site (Experimental Procedures). For a given distance to the LFP recording site (x axis), we considered all MUA sites that were within that distance to the electrode and computed the correlation coefficient between the LFP response and the average normalized MUA signal (filled squares). The open squares denote a similar procedure but using only those sites that were farther than the corresponding distance to the LFP recording site and within a maximum distance of 12 mm. Error bars denote SEM.

Because this analysis suggests that LFP selectivity is related to neuronal signals on a spatial scale of  $\sim 3$  mm and it has been argued that LFPs might “listen” to activity over a much greater spatial distance than spikes (Beard et al., 2004; Juergens et al., 1999; Mitzdorf, 1985), we sought to better understand the spatial organization within IT. Previous work showed that there is a spatial organization of stimulus selectivity in IT cortex such that the spikes of nearby IT neurons prefer similar visual shapes (Fujita et al., 1992; Gochin et al., 1991). To re-examine the spatial organization of spiking activity with our stimulus set, we compared the MUA-determined object preferences at pairs of sites (1) recorded along the same penetration (i.e., moving the electrode approximately normal through ventral IT cortex in steps of 100 or 200  $\mu\text{m}$ ; Figure S6) and (2) recorded on different penetrations (i.e., approximately horizontal displacements along the ventral IT cortex, Experimental Procedures).

We often observed that stimulus preferences measured by spike counts remained similar along the same penetration. For example, for the penetration shown in Figure S5, the MUA recorded upon entry into IT preferred images of cats and dogs. At least four subsequent sites recorded several hundred microns apart from this one also showed enhanced firing rates for some images of cats and dogs. A site recorded 800  $\mu\text{m}$  away from the first one showed enhanced activity for one dog and one vehicle, while another site 1000  $\mu\text{m}$  away showed a weak selective response to the same vehicle, and another site 1200  $\mu\text{m}$  away preferred cats and dogs.

The similarity of MUA-determined stimulus preferences at nearby sites illustrated in Figure S5 was not observed in every penetration. We quantified the similarity of stimulus preferences at spatially separate pairs of recording sites as the Pearson correlation between the

mean responses to each of the 77 images. The average object preference similarity for the MUA responses from pairs of selective sites within the same penetration (0.28) was significantly higher than for pairs of selective sites from different penetrations (0.02; *t* test,  $p < 10^{-10}$ ). To more closely examine the relationship of spatial distance and stimulus preference similarity, we determined the stimulus preference similarity as a function of the distance between sites. Figure 7A shows that, on average, there is strong stimulus preference similarity in the MUA response as far as 800  $\mu\text{m}$  apart along the same penetration through IT. We also observed a strong similarity between the responses of different single units recorded from the same electrode (Gochin et al., 1991) and between SUA and MUA from the same electrode (data not shown). Similarity of stimulus preferences within 200  $\mu\text{m}$  is perhaps not surprising, because MUA likely reflects the spiking activity of neurons in a sphere of approximately that radius around the electrode tip (Holt and Koch, 1999; Logothetis, 2003), and the MUA signal band typically appeared to be dominated by a small number of spiking neurons based on the spike-sorting results. However, the similarity of MUA-determined stimulus preferences at distances as far as 800  $\mu\text{m}$  (Figure S5 and Figure 7A) strongly supports the hypothesis of spatial organization in IT (i.e., clusters of neurons with similar object preferences; Fujita et al., 1992; Wang et al., 1996). The similarity of MUA-determined stimulus preferences is not seen for sites separated horizontally by 1 mm or more (Figure 7B), consistent with the suggestion of  $\sim 500 \mu\text{m}$  as determined by tangential penetrations through IT (Fujita et al., 1992). Similar observations were made with SUA (Figure S7).

The LFP-determined stimulus preference similarities showed a spatial pattern that extended over a much larger spatial scale than the MUA-determined similarities (Figure 7). LFP-determined stimulus preferences were more similar than the MUA-determined stimulus preferences at all distances along the penetration (cf. Figures 7A and 7C). Moreover, in contrast to spiking activity, the LFP-determined stimulus preferences showed significant correlation at horizontally separated sites. Care should be taken in the interpretation of correlation coefficients obtained from comparisons across separate sessions. In particular, distances measured from sites in separate penetrations may have large errors on the order of 1 mm (Nahm et al., 1994). In spite of these caveats, we observed that the degree of similarity fell off gradually over several millimeters. LFP recording sites that are separated by less than 5–8 mm showed at least partial correlation in their stimulus preferences (Figure 7D). These observations are not due to computing correlation coefficients across very distinct classes of stimuli, because we confirmed these results when computing the similarity across sites for objects *within* each of the different classes of objects that we used in this study (Figure S8). We simulated errors in the distance measurements across penetrations, and we observed that the results shown in Figures 6 and 7D are robust to errors of a few millimeters (Supplemental Data). The similarity in LFP responses across large distances probably reflects a combination of large-scale similarity in the dendritic input to IT neurons and the larger spread of the LFP signal.

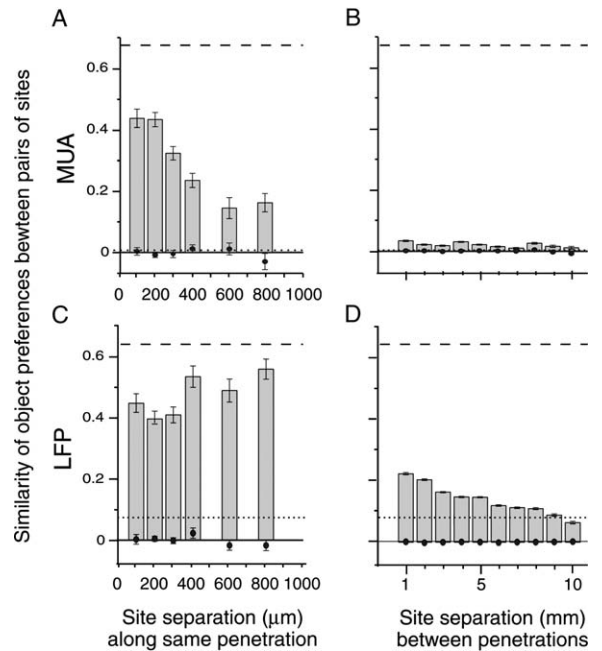


Figure 7. Similarity of Stimulus Preferences versus Distance between Sites

For all panels, the ordinate shows the mean Pearson correlation coefficients between responses to all 77 images at spatially separate sites as a function of the separation distance. For recording sites within the same penetration (A and C), the distance between each pair of sites was determined by the microdrive readings along the penetration; for recording sites in different penetrations (B and D), the distance was determined from the anterior/posterior and lateral/medial locations of the penetrations at the cortical surface (Experimental Procedures). (A and B) Similarity of MUA-determined stimulus preferences for pairs within the same penetration (A) and different penetrations (B). (C and D) Similarity of LFP-determined stimulus preferences for pairs within the same penetration (C) and different penetrations (D). Error bars correspond to SEM. Black dots show the mean correlation computed using the responses in the 100 ms interval before stimulus onset. For all plots, only sites that showed a statistically significant response were included in each pair. The number of penetrations that contributed to the plots was 86 in part (A) and 64 in part (C). The number of site pairs differed among the separate columns in the plots (range = 35 to 2030). As an estimate of the maximum correlation that could be expected given the variability in the data, the dashed horizontal lines show the mean correlation obtained from comparing the odd and even repetitions of the MUA versus MUA (A and B) or LFP versus LFP (C and D) at the same site (Experimental Procedures). The dotted line shows the correlation coefficient between sites in different hemispheres.

## Discussion

We studied the properties of the ensemble input to IT cortex in monkeys by measuring the LFPs. We observed that LFPs often showed selectivity to complex visual stimuli and also showed tolerance to changes in image position and scale. Spiking activity (both multi-unit activity and single-unit activity) showed stronger selectivity both in terms of the number of selective sites and the sharpness of selectivity. Upon directly comparing the lower frequencies of the LFP and the spiking responses, we observed only a weak similarity of the object preferences at each site. However, the LFP object selectivity was better explained by a simple model that combined the spiking response in an area of several millimeters

around the LFP recording site. Analysis of object selectivity at spatially separate pairs of sites suggested that both MUA and LFP signals are spatially organized in IT, but that LFP signals may be organized on a larger spatial scale. These observations provide evidence that synaptic input to IT neurons convey position- and size-tolerant selectivity for complex shapes and that such synaptic input may have an underlying spatial organization on a spatial scale spanning several millimeters.

### Stimulus Selectivity of LFPs in IT Cortex

Given that the LFP constitutes an ensemble response over relatively large cortical areas, probably spanning several millimeters (Juergens et al., 1999; Mitzdorf, 1985), we were surprised to observe that the LFPs from a large fraction of IT sites were selective across our arbitrary set of stimuli. Many previous studies have reported such stimulus selectivity in the spiking response of IT at the MUA or SUA level (Gochin et al., 1991; Gross et al., 1972; Logothetis and Sheinberg, 1996; Perrett et al., 1982; Schwartz et al., 1983; Tanaka, 1996), but we are not aware of any previous study that has shown that LFPs in IT are also stimulus selective. Selective LFP responses have been observed in other brain areas, such as motor cortex (Donchin et al., 2001; Mehring et al., 2003), cat visual cortex (Mitzdorf, 1985), macaque parietal cortex (Pesaran et al., 2002; Scherberger et al., 2005), macaque earlier visual areas (Fries et al., 2001; Logothetis, 2003), and the occipito-temporal lobe of epileptic human patients (Allison et al., 1994).

The LFP signal is the result of multiple sources. Calculations of propagating electric fields in the extracellular milieu indicate that signals below 300 Hz could arise from several hundred microns to tens of millimeters away from the electrode (with lower frequencies propagating farther than higher frequencies (Bedard et al., 2004; Logothetis, 2003; Mitzdorf, 1985)). Because of this summation, temporally coincident sources will more strongly contribute to the LFP signal. Possible sources include dendritic potentials, afterhyperpolarizations, afterdepolarizations, axonal spikes, somatic spikes, and glial activity. The contribution from glial activity, capacitive components, and spikes is thought to be relatively small (Mitzdorf, 1985) (except for the ~100–300 Hz frequency band that likely contains power resulting from nearby action potentials (Logothetis, 2003)). Excitatory postsynaptic potentials in dendrites likely constitute an important component of the LFP signal (Mitzdorf, 1985). Thus, the LFP signal can roughly be thought of as a spatially and temporally low-pass filtered measurement of the coincident dendritic potentials in a cortical region.

Given this, the most straightforward explanation of our observation that LFPs in IT are stimulus selective is that (1) the pattern of dendritic activity in IT (e.g., that arising from posterior IT, V4, and intracortical processing) is different for different visual stimuli and (2) that there is either some spatial organization to that dendritic activity or that components of that activity are more synchronous for some stimuli than for others, or both. Nonetheless, LFPs must be interpreted cautiously: while spikes represent a signal that is directly responsible for neurotransmitter release and may be conveyed to other brain regions, LFPs represent a signal combined in

a nonstraightforward way over many neurons. Although this combined response often shows visual selectivity, unlike spikes, it likely does not represent a signal that is directly used by the brain or targets of IT to support object discrimination.

The observation that LFPs show tolerance to changes in object scale and position suggests that these properties may be present in the synaptic input to IT, as suggested by spike recordings in earlier areas along the visual pathway (Pasupathy and Connor, 1999; Gustavsen and Gallant, 2003) and by computational theories of object recognition (Riesenhuber and Poggio, 1999). The local spiking signals show stronger and sharper selectivity. This could be due to the spatial averaging of the LFP signal and to the nonlinear transformations of excitatory potentials into spikes, which constitute a fundamental step in the computations involved in discriminating different objects.

### Comparison of MUA and LFP Selectivity in IT Cortex

The relationship of spike responses to LFPs in cortical tissue is particularly interesting in light of the large volume of fMRI work in humans and other species. Recent studies in monkeys by Logothetis and colleagues showed that fMRI BOLD correlates better with the LFP than with spiking activity (Logothetis, 2003; see also Kayser et al., 2004; Mathiesen et al., 2000). Several investigators reported different degrees of covariation between spiking signals and LFPs. In several cases, spikes were reported to fire at specific phases with respect to the LFPs (Donchin et al., 2001; Eggermont and Mossop, 1998; Fries et al., 2001; Murthy and Fetz, 1996; Pesaran et al., 2002; Scherberger et al., 2005).

We found that LFP stimulus preferences can be similar to spiking preferences, but at most sites this similarity was weak. In light of the arguments presented above, spikes and LFPs likely constitute different signals in terms of their neural origins and spatial resolution. The difference in stimulus preferences could reflect differences between the synaptic inputs to (LFP) and the outputs of pyramidal neuron spiking activity within each piece of IT cortex. Such differences are expected, as the processing of synaptic inputs within IT cortex likely involves complex nonlinear processes between activity in large dendritic trees and spiking output (including local interneuron processing). In addition, because the LFP frequency range likely reflects a spatial average over larger distances than the spikes (~200  $\mu\text{m}$  versus mm), even if the dendritic potentials at each cortical point had the same stimulus preferences as the spiking activity at that point, one would expect differences between LFP and spike stimulus preferences.

### Spatial Organization in the Synaptic Input and Output of IT

Interestingly, a simple model that averages the spiking signals within an area of several millimeters around the LFP recording site could explain the LFP signal better than using only the spikes on the same electrode (cf. Figure 6 versus Figure 5B). Sites farther than 3–5 mm from the LFP recording site contributed comparatively little to the LFP signal (Figure 6). This suggests that the selectivity in the LFP signal could be related to the topographical arrangement in the spatial organization of

selective neurons and/or the organization of the dendritic activity of those neurons.

Topographical organization of the output spiking activity is prominent throughout cortex (Mountcastle, 1957) and has also been demonstrated in IT cortex (Fujita et al., 1992; Tanaka, 2003). Consistent with this, we here report strong similarity in the stimulus preferences of spiking activity at sites within the same penetration (Figure 7A and Figures S5–S8). With MUA data obtained from a single electrode, it is hard to rigorously establish that the recordings separated by 200  $\mu\text{m}$  or less actually correspond to separate neurons. However, we verified our observations of topography also at the level of SUA (Figure S7), and therefore the spatial organization that we observed cannot be attributed to a more diffuse nature of MUA. Furthermore, we observed that correlations in the spiking responses extend beyond 400  $\mu\text{m}$  (in some cases even beyond 800  $\mu\text{m}$ , e.g., Figure S5), and simulation studies indicate that extracellular signals arising from somatic spikes are likely too small to record when the electrode is more than 200  $\mu\text{m}$  away from the cell body (Holt and Koch, 1999; Logothetis, 2003).

These observations support the notion that there is a spatial organization in the representation of visual information in the spiking output of IT (Fujita et al., 1992; Gochin et al., 1991). What about the synaptic input to IT neurons? We observed that sites that were several millimeters apart maintained some similarity in the LFP stimulus preferences (Figure 7D). This agrees with other estimates of the spatial extent of LFP recordings (Juegens et al., 1999; Logothetis, 2003; Mitzdorf, 1985). For example, Murthy and Fetz reported that sites separated by up to 14 mm in precentral cortex showed significant correlation in the LFP activity in the 20–40 Hz band (Murthy and Fetz, 1996). The long spatial range of similarity of LFP stimulus preferences might reflect an organization in IT over a scale of several millimeters (e.g., perhaps a spatial organization of the axonal synaptic inputs to IT, dendritic spreads of IT neurons, or horizontal connections). However, we remain cautious about such a hypothesis because of two other possible interpretations: (1) the long-range correlations could also be partly due to overall biases in the LFP preferences for different stimuli within our set; (2) sources in the LFP frequency range can theoretically be recorded over larger spatial distances (Bedard et al., 2004; Mitzdorf, 1985). The non-zero correlation in LFP signals across hemispheres (dotted line in Figure 7D) probably reflects the contribution of the stimulus bias. Thus, the correlations observed up to the 5 mm range are probably a combination of a topography in the synaptic input to IT neurons and the long range at which LFP signals can be “heard” by the electrode. With our current data, it is difficult to distinguish the relative contributions of these two explanations.

Understanding the nonlinear transformations of dendritic input to output in IT cortex constitutes one of the most important challenges to understand the computations involved in solving the fundamental problem of object recognition. Here we showed that the LFP in IT cortex shows position- and scale-tolerant selectivity to complex visual objects, and we suggest that the synaptic input to IT neurons is topographically organized on a scale of several millimeters.

## Experimental Procedures

### Stimuli and Task

We used 77 grayscale images (Figure 1 and Figure S1). Stimuli were presented on a video monitor ( $52^\circ \times 34^\circ$ , 75 Hz,  $1600 \times 1200$  pixels, background gray of 28  $\text{cd}/\text{m}^2$ ) positioned 52 cm from the monkey. Images had a  $3.4^\circ$  width (130 pixels). Images were not normalized for gray level or contrast: peak luminance ranged from 0.5 to 57  $\text{cd}/\text{m}^2$ . Animals fixated on a  $0.2^\circ$  red fixation point (fixation window of  $\pm 2^\circ$ ). During each trial, 20 stimuli were presented at the fixation point at five stimuli per second (seven frames on [93 ms], interleaved by seven frames of background). Stimuli were presented in pseudo-random order, with one entire set of images presented before beginning the next. Each image was shown ten times. In addition to the 77 images, one “blank” stimulus (i.e., consisting of entirely background gray pixels) was included in these presentation sequences. To study the degree of tolerance to scale and position changes, the 77 images were presented at two additional scales (twice the size and half the size) and two additional positions ( $2^\circ$  and  $4^\circ$  from the center of gaze along the contralateral horizontal meridian).

### Surgical Preparation and Electrophysiological Recordings

Recordings were made from two monkeys (*Macaca mulatta*) weighing 6.0 kg (monkey K, female) and 5.0 kg (monkey N, male). Aseptic surgery was performed to attach a head post to the skull and to implant a scleral search coil in one eye. After  $\sim 2$  months of behavioral training, a second surgery was performed to place a recording chamber (centered at Horsley-Clark coordinates A 16, L 12; guided by MR images of each monkey) to reach the anterior portion of right inferotemporal cortex. A second chamber was implanted to reach the left AIT of monkey K after 1 year of recording. Recordings were made from both hemispheres of monkey K and the right hemisphere of monkey N. A 26G guide tube was inserted to reach  $\sim 20$  mm above AIT from a dorsal approach (all electrodes were sharp, glass-coated Pt/Ir; 0.5–1.5  $\text{M}\Omega$  at 1 kHz). The superior temporal sulcus (STS) and the ventral surface were identified by comparing gray and white matter transitions and the depth of the skull base with structural MR images. Penetrations were made over an  $\sim 10 \times 10$  mm area of the ventral surface (Horsley-Clark AP, 10–20 mm; ML, 14–24 mm). We made estimates of electrode penetrations and recording site locations based on MR images taken after chamber implantation. Electrode penetrations were spaced 1 mm apart by using a fixed grid at the surface of the skull. The coronal sections at A16 are shown with recording sites for A15–A17 in Figure S6. The voltage on the electrode relative to a large grounding area on the skull (the headpost) was amplified (Bak Electronics, Mount Airy, MD) and split into two signals (Krohn-Hite Corp., Brockton, MA). One band (400 Hz to 6 kHz; 8-pole Bessels) was used to examine spiking activity. The second band (1–300 Hz; 8-pole Butterworth) was defined as the LFP waveform (sampled at 1 kHz).

### Data Analysis

We recorded from 598 sites in the ventral surface of AIT (LFP were recorded from 506 sites). The spike response was defined as the spike count in the 100–200 ms interval after stimulus onset, and LFP response was defined as the total power in the same interval. In Figure 5B and Figure S3, we compared different definitions of spike and LFP responses. In Figure 5C, the LFP response was based on power in different frequency bands (Press et al., 1996). Preprocessing consisted of the following steps. Trials where the monkey broke fixation were discarded. Responses from the first three presentations in each trial were not analyzed. For the LFP, we applied a digital notch filter at 60 Hz and harmonics (fourth-order elliptic filter, 0.1 db peak-to-peak ripple, 40 db stopband attenuation). We computed the power spectral density by use of the Welch method (Figure S2A) with a 256 point Hanning window using a 10 point overlap (Press et al., 1996). Most of the spectral power was concentrated below 40 Hz ( $82\% \pm 22\%$  of the total power). We discarded sites that showed peaks at harmonics of 60 Hz or high-frequency noise in the LFPs (12 sites for spikes and 108 sites for LFPs). We considered the change in response versus repetition number (longer-term stationarity). A site was not considered further if the change in response with time was  $>30\%$  (MUA, 166; LFP, 62 sites). The short-term stationarity was assessed by averaging over all the first pictures in each

trial, all the second pictures, and so on, and then computing the slope of response versus presentation order (this step removed 4.5% of recording sites for spikes and 3.2% for LFPs). We obtained a final set of 315 reliable LFP sites and 364 reliable MUA sites (249 common sites). The spike waveforms were submitted to a spike-sorting algorithm to yield 170 units with SUA (Quian Quiroga et al., 2004).

The sparseness index used in Figure 3B was defined as

$$\frac{\left(\sum_{i=1}^{77} r_i / 77\right)^2}{\sum_{i=1}^{77} r_i^2 / 77}$$

(Rolls and Tovee, 1995). To assess the selectivity of each recording site, we used a nonparametric ANOVA comparing the variance of the responses across different stimuli ( $\sigma^2_{\text{across}}$ ) with the trial-by-trial response variance to the same stimulus ( $\sigma^2_{\text{within}}$ ). The ratio of these variances ( $r_v = \sigma^2_{\text{across}} / \sigma^2_{\text{within}}$ ) was taken as an index of the sharpness of selectivity. To test significance, we estimated the empirical distribution of  $r_v$  under the null hypothesis of equal responses to all images by shuffling the image labels. To assess nonspecific effects due to nonstationarity or poor randomization, we repeated all analyses in a control interval defined as the 100 ms before stimulus onset. To assess whether the selectivity could be explained by low-level image properties, we computed the percentage of variance explained by 16 simple properties of each image with the mean spike or LFP response to that image (mean pixel intensity, SD of pixel intensity, SD/mean of pixel intensity, number of nongray pixels, number of bright and dark pixels with different thresholds for bright/dark, number of nonblack pixels, mean pixel intensity within the object, SD pixel intensity within the object, minimum and maximum pixel intensity within the object, pixel intensity range, contrast, and total power). We compared the similarity of stimulus preferences at different recording sites (Figure 7) and between spikes and LFP (Figures 5 and 6) by computing the Pearson correlation coefficient between 77 dimensional vectors containing the mean responses to each image. For comparison, we also computed the correlation coefficient between even and odd repetitions of the MUA or LFP responses to provide a measure of the variability responses. Because the latter correlation coefficients were obtained from five repetitions instead of ten, we report the values obtained by extrapolation assuming independence of the noise in separate repetitions.

We built a simple model by computing the average spiking activity in a large cortical area. For a given location  $L$ , the resulting signal was

$$y_L = \frac{1}{n} \sum_{d \leq r} \frac{s_d}{(1 + d/a)}$$

where  $s_d$  is the normalized spike response at a site separated by a distance  $d$  to location  $L$ ,  $n$  is the total number of sites within the sphere of radius  $r$ , and  $a$  is a scale parameter that weights the signal to emphasize nearby points. We compared the results for different values of  $a$ , and we did not observe significant differences, and therefore we report the values for  $a = \infty$  (i.e., no weight) condition. The output of this model is a vector with a response value for each of the 77 images. This signal was then compared to the LFP signal by using the Pearson correlation coefficient, as was done for the other spike versus LFP comparisons.

#### Supplemental Data

The Supplemental Data for this article can be found online at <http://www.neuron.org/cgi/content/full/49/3/433/DC1/>.

#### Acknowledgments

We would like to thank Alec Shkolnik for initial help with the analysis; Nancy Kanwisher, Christof Koch, John Maunsell, Tony Movshon, and Peter Schiller for comments on the manuscript and helpful discussion; and CSBi for computer cluster usage. We also thank J. Patrick Mayo and Jennifer Deutsch for animal husbandry and technical support. This research was sponsored by The Defense Advanced

Research Projects Agency, The Office of Naval Research (DARPA/ONR N00014-02-1-0915), NIH, and a Whiteman Fellowship to G.K.

Received: June 14, 2005

Revised: September 8, 2005

Accepted: December 15, 2005

Published: February 1, 2006

#### References

- Allison, T., Ginter, H., McCarthy, G., Nobre, A.C., Puce, A., Luby, M., and Spencer, D.D. (1994). Face recognition in human extrastriate cortex. *J. Neurophysiol.* **71**, 821–825.
- Bedard, C., Kroger, H., and Destexhe, A. (2004). Modeling extracellular field potentials and the frequency-filtering properties of extracellular space. *Biophys. J.* **86**, 1829–1842.
- DiCarlo, J., and Maunsell, H. (2000). Form representation in monkey inferotemporal cortex is virtually unaltered by free viewing. *Nat. Neurosci.* **3**, 814–821.
- Donchin, O., Gribova, A., Steinberg, O., Bergman, H., Cardoso de Oliveira, S., and Vaadia, E. (2001). Local field potentials related to bi-manual movements in the primary and supplementary motor cortices. *Exp. Brain Res.* **140**, 46–55.
- Eggermont, J.J., and Mossop, J.E. (1998). Azimuth coding in primary auditory cortex of the cat. I. Spike synchrony versus spike count representations. *J. Neurophysiol.* **80**, 2133–2150.
- Felleman, D.J., and Van Essen, D.C. (1991). Distributed hierarchical processing in the primate cerebral cortex. *Cereb. Cortex* **1**, 1–47.
- Fries, P., Reynolds, J., Rorie, A., and Desimone, R. (2001). Modulation of oscillatory neuronal synchronization by selective visual attention. *Science* **293**, 1560–1563.
- Fujita, I., Tanaka, K., Ito, M., and Cheng, K. (1992). Columns for visual features of objects in monkey inferotemporal cortex. *Nature* **360**, 343–346.
- Fukushima, K. (1980). Neocognitron: a self organizing neural network model for a mechanism of pattern recognition unaffected by shift in position. *Biol. Cybern.* **36**, 193–202.
- Gochin, P., Miller, E., Gross, C., and Gerstein, G. (1991). Functional interactions among neurons in inferior temporal cortex of the awake macaque. *Exp. Brain Res.* **84**, 505–516.
- Grill-Spector, K., and Malach, R. (2004). The human visual cortex. *Annu. Rev. Neurosci.* **27**, 649–677.
- Gross, C.G. (1994). How inferior temporal cortex became a visual area. *Cereb. Cortex* **5**, 455–469.
- Gross, C., Rocha-Miranda, C., and Brender, D. (1972). Visual properties of neurons in inferotemporal cortex of the Macaque. *J. Neurophysiol.* **35**, 96–111.
- Gustavsen, K., and Gallant, J.L. (2003). Shape perception: complex contour representation in visual area V4. *Curr. Biol.* **13**, R234–R235.
- Haberly, L., and Shepherd, G. (1973). Current-density analysis of summed evoked potentials in opposum prepyriform cortex. *J. Neurophysiol.* **36**, 789–803.
- Haxby, J.V., Gobbini, M.I., Furey, M.L., Ishai, A., Schouten, J.L., and Pietrini, P. (2001). Distributed and overlapping representations of faces and objects in ventral temporal cortex. *Science* **293**, 2425–2430.
- Hodgkin, A.L., and Huxley, A.F. (1952). A quantitative description of membrane current and its application to conduction and excitation in nerve. *J. Physiol.* **117**, 500–544.
- Holt, G.R., and Koch, C. (1999). Electrical interactions via the extracellular potential near cell bodies. *J. Comp. Neurosci.* **6**, 169–184.
- Ito, M., Tamura, H., Fujita, I., and Tanaka, K. (1995). Size and position invariance of neuronal responses in monkey inferotemporal cortex. *J. Neurophysiol.* **73**, 218–226.
- Juergens, E., Guettler, A., and Echhorn, R. (1999). Visual stimulation elicits locked and induced gamma oscillations in monkey intracortical and EEG-potentials but not in human EEG. *Exp. Brain Res.* **129**, 247–259.

- Kanwisher, N., McDermott, J., and Chun, M.M. (1997). The fusiform face area: a module in human extrastriate cortex specialized for face perception. *J. Neurosci.* *17*, 4302–4311.
- Kayser, C., Kim, M., Ugurbil, K., Kim, D.S., and Konig, P. (2004). A comparison of hemodynamic and neural responses in cat visual cortex using complex stimuli. *Cereb. Cortex* *14*, 881–891.
- Keysers, C., Xiao, D.K., Foldiak, P., and Perret, D.I. (2001). The speed of sight. *J. Cogn. Neurosci.* *13*, 90–101.
- Koch, C. (1999). *Biophysics of Computation* (New York: Oxford University Press).
- Kreiman, G. (2004). Neural coding: computational and biophysical perspectives. *Physics of Life Reviews* *1*, 71–102.
- Logothetis, N.K. (2003). The underpinnings of the BOLD functional magnetic resonance imaging signal. *J. Neurosci.* *23*, 3963–3971.
- Logothetis, N.K., and Sheinberg, D.L. (1996). Visual object recognition. *Annu. Rev. Neurosci.* *19*, 577–621.
- Mathiesen, C., Caesar, K., and Lauritzen, M. (2000). Temporal coupling between neuronal activity and blood flow in rat cerebellar cortex as indicated by field potential analysis. *J. Physiol.* *523*, 235–246.
- Mehring, C., Rickert, J., Vaadia, E., Cardoso de Oliveira, S., Aertsen, A., and Rotter, S. (2003). Inference of hand movements from local field potentials in monkey motor cortex. *Nat. Neurosci.* *6*, 1253–1254.
- Mitzdorf, U. (1985). Current source-density method and application in cat cerebral cortex: investigation of evoked potentials and EEG phenomena. *Physiol. Rev.* *65*, 37–99.
- Mountcastle, V.B. (1957). Modality and topographic properties of single neurons of cat's somatic sensory cortex. *J. Neurophysiol.* *20*, 408–434.
- Murthy, V.N., and Fetz, E.E. (1996). Oscillatory activity in sensorimotor cortex of awake monkeys: synchronization of local field potentials and relation to behavior. *J. Neurophysiol.* *76*, 3949–3967.
- Nahm, F.K., Dale, A.M., Albright, T.D., and Amaral, D.G. (1994). In vivo microelectrode localization in the brain of the alert monkey: a combined radiographic and magnetic resonance imaging approach. *Exp. Brain Res.* *98*, 401–411.
- Pasupathy, A., and Connor, C. (1999). Responses to contour features in macaque area V4. *J. Neurophysiol.* *82*, 2490–2502.
- Perrett, D., Rolls, E., and Caan, W. (1982). Visual neurones responsive to faces in the monkey temporal cortex. *Exp. Brain Res.* *47*, 329–342.
- Pesaran, B., Pezaris, J., Sahani, M., Mitra, P., and Andersen, R. (2002). Temporal structure in neuronal activity during working memory in macaque parietal cortex. *Nat. Neurosci.* *5*, 805–811.
- Press, W.H., Teukolsky, S.A., Vetterling, W.T., and Flannery, B.P. (1996). *Numerical Recipes in C, Second Edition* (Cambridge: Cambridge University Press).
- Quian Quiroga, R., Nadasdy, N., and Ben-Shaul, Y. (2004). Unsupervised spike sorting with wavelets and superparamagnetic clustering. *Neural Comput.* *16*, 1661–1687.
- Richmond, B., Wurtz, R., and Sato, T. (1983). Visual responses in inferior temporal neurons in awake Rhesus monkey. *J. Neurophysiol.* *50*, 1415–1432.
- Riesenhuber, M., and Poggio, T. (1999). Hierarchical models of object recognition in cortex. *Nat. Neurosci.* *2*, 1019–1025.
- Rolls, E.T., and Tovee, M.J. (1995). Sparseness of the neuronal representation of stimuli in the primate temporal visual cortex. *J. Neurophysiol.* *73*, 713–726.
- Sato, T., Kawamura, T., and Iwai, E. (1980). Responsiveness of inferotemporal single units to visual pattern stimuli in monkeys performing discrimination. *Exp. Brain Res.* *38*, 313–319.
- Scherberger, H., Jarvis, M.R., and Andersen, R.A. (2005). Cortical local field potential encodes movement intentions in the posterior parietal cortex. *Neuron* *46*, 347–354.
- Schwartz, E., Desimone, R., Albright, T., and Gross, C. (1983). Shape-recognition and inferior temporal neurons. *Proc. Natl. Acad. Sci. USA* *80*, 5776–5778.
- Tanaka, K. (1996). Inferotemporal cortex and object vision. *Annu. Rev. Neurosci.* *19*, 109–139.
- Tanaka, K. (2003). Columns for complex visual object features in the inferotemporal cortex: clustering of cells with similar but slightly different stimulus selectivities. *Cereb. Cortex* *13*, 90–99.
- Wallis, G., and Rolls, E.T. (1997). Invariant face and object recognition in the visual system. *Prog. Neurobiol.* *51*, 167–194.
- Wang, G., Tanaka, K., and Tanifuji, M. (1996). Optical imaging of functional organization in the monkey inferior temporal cortex. *Science* *272*, 1665–1668.